

## Alternative ion-ion pair-potential model applied to molecular dynamics simulations of hot and dense plasmas: Al and Fe as examples

Yong Hou and Jianmin Yuan\*

*Department of Physics, National University of Defense Technology, Changsha 410073, China*

(Received 1 September 2008; revised manuscript received 11 November 2008; published 8 January 2009)

A model to calculate the ion-ion pair potentials in hot and dense plasmas is developed based on temperature-dependent density functional theory. The electronic structures, including the energy level and space distributions, are calculated using an average-atom model. The calculated electron space number density is divided into two parts: one is a uniformly distributed electronic sea  $\rho(r_b)$  with a density equal to the total electronic density at the ion sphere boundary, which is redistributed when space overlap occurs between the interacting ions; the left part of the electronic density  $\rho_i^{2nd}(r)$  represents the dramatic space variations of the electrons due to the nuclear attraction and the shell structure of the bound states, which maintains unchanged during the interactions between the ions. The pair potential is obtained through space integrations for the energy density functions of electron density. We present molecular dynamics simulations for the ion motion on the basis of the calculated pair potentials in a wide regime of density and temperature. As an example, hot and dense Al and Fe plasmas are simulated to give the equation of state and ion-ion pair distribution function. The results are in agreement with those of other theoretical models.

DOI: [10.1103/PhysRevE.79.016402](https://doi.org/10.1103/PhysRevE.79.016402)

PACS number(s): 52.25.Kn, 51.30.+i, 95.30.Tg, 34.20.Cf

### I. INTRODUCTION

With the development of laser techniques, it is possible to produce hot and dense plasmas in the laboratory, and theoretical models of the structures of this kind of matter are necessary to simulate properties such as equations of state, radiative transfer coefficients, and conduction coefficients. These kinds of properties are important in inertial confinement fusion (ICF) and astrophysics researches and the electronic structure of matter determines most of these properties. Many efforts have been devoted to investigate the electronic structure. The Thomas-Fermi (TF) [1–3] model is the simplest statistical model, which treats the electrons as local quantum free-electron gases with the local density of the electrons depending on the effective potential of the electrons moving in. The Thomas-Fermi-Dirac (TFD) [4] model was designed in a relativistic form on the basis of the TF model. The average-atom (AA) model [5–8] was developed to describe bound electrons with the well-known one-electron shell structure model and ionized electrons with the TF statistical model. These models were used to describe the electronic structures of hot and dense plasmas in most cases with the assumption of a single-particle spherically symmetric ionic potential. The density effects were considered by using an ion sphere with finite sizes. However, in the region of strongly coupled plasmas, the ion-ion interactions could break the spherically symmetric ionic potential, and so one must consider the effects implicitly. The effective interionic potentials used to describe the nuclear motions in the plasma cannot be approximated reasonably by most models used in normal cases, such as the Lennard-Jones potential one usually employs at room temperature. In particular, when large ionization of the atoms at high temperature and density happens, the potentials would have big differences compared

with the empirical ones obtained in normal conditions. The *ab initio* molecular dynamics technique [9] considers the electronic structures as a function of the internuclear coordinates and does not need to calculate the pair potential between atoms or ions. However, this kind of *ab initio* simulation can only be performed at low temperatures [10]. Dharma-wardana and Perrot [11] solved the Kohn-Sham equation for the electrons in the frame of density-functional theory (DFT) and treat interionic correlations using the hypernetted-chain (HNC) approximation, and then Dharma-wardana and Murillo [12] applied the method to the two-temperature, two-mass system. Ofer *et al.* [13] proposed the TF HNC model in which the Kohn-Sham equation is replaced by the TF statistical approximation for electrons and the HNC approximation for interionic correlations. Furukawa and Nishihara [14] constructed a model based on the AA model to calculate the cross sections and the rate coefficients of atomic processes including ion-ion correlation effects within the framework of the quantal hypernetted-chain (QHNC) approximation. Zérah and co-workers [15–18] proposed a Thomas-Fermi molecular dynamics (TFMD) scheme, in which the electronic kinetic and entropy parts of the free energy are expressed implicitly in terms of the electron density through the TF functional and combined with a molecular dynamics for ions. Salzmann and Fisher [19] presented an ion ellipsoid model (IEM). In that model, the ion is confined to an ellipsoidal enclosure, and the statistical distributions of the ellipsoids' shapes and sizes and the electric field distributions are described in good agreement with Monte Carlo results with a plasma coupling constant from 0 to 16. Rozsnyai *et al.* [20] calculated the Al and Be atoms in the solid or liquid state using the quantum-mechanical model at finite temperatures and gave good Hugoniot data compared with the experimental results in the warm dense regime. They all tried to solve the nuclear and electronic distributions simultaneously.

In the present study, classical molecular dynamics simulations are carried out for the ion motions and a modified AA

\*Corresponding author: [jmyuan@nudt.edu.cn](mailto:jmyuan@nudt.edu.cn)

model [8] is solved to describe the electronic distribution. The ion-ion pair potentials are obtained from the electronic densities' overlap of two isolated ions based on a modified temperature- and density-dependent Gordon and Kim (GK) [21] theory. The GK theory was originally proposed to calculate the interatomic or intermolecular potential and has been applied widely to ionic crystal [22] systems and noble-gas atoms. The results obtained from the theory had been found to give excellent agreement with the known structures and binding energies [23,24]. However, these calculations were based on the electron density distribution of the free atoms or ions on the ground states, and the pair potentials obtained were only applied to closed-shell atomic systems without considering the temperature effect on the electronic level occupations and density space distributions. In the present model, the temperature and density effects on the interionic potentials in hot and dense plasmas are considered by using a modified AA model [8,25] to include the thermal electronic excitations and ionizations in a statistical way. The rearrangement of the nonlocal free electrons, when the interacting ions come together, is also considered by retaining the total space volume of the interacting system unchanged during the interaction.

## II. METHOD OF CALCULATION

In the GK [21] theory, the total energy of the system consists of the direct Coulomb potential energy, the exchange Coulomb potential energy, the kinetic energy, and the correlation energy. The direct Coulomb potential energy is calculated by integrating the Coulomb potential over the space distribution of the electron density, while the other three energies are calculated by using a temperature-dependent local density functional approximation (LDA); i.e., the energy calculation needs only approximate energy density functionals and the electron density space distribution. The interaction potential is the total energy difference between the whole system (with space overlap) and the separate systems (without space overlap). We obtain the electronic density by using a modified AA model [8,25] to include the temperature and density effects on the electronic distributions in a statistical way. The electronic density is divided into two parts: the nonlocal uniformly distributed free-electron sea  $\rho(r_b)$  in the whole space with a density equal to the density of electrons at the ion sphere boundary,  $r_b$ , and the local electrons  $\rho_i^{2nd}(r)$  representing the dramatic space variation of the electronic distribution around the nucleus. For each isolated ion, the local electron density is the total density minus the nonlocal free-electron density and is assumed to be unchanged during the interaction. As shown in Fig. 1, the space distribution of the nonlocal free electrons representing by the region with the closed solid line changes when two interacting ions come together, but the space volume of the region retains unchanged, resulting in unchanged uniformly distributed nonlocal free electrons, while the localized electrons distributed in the dashed line rounded region overlap each other, with the density of the total local electrons being the sum of the separate ions in the overlap region. When two nuclei come closer the localized electrons

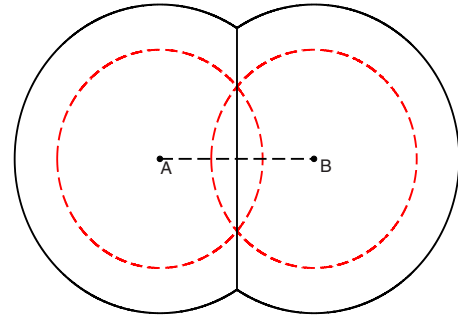


FIG. 1. (Color online) Space distribution of the nonlocal free-electron sea  $\rho_i(r_b)$  (surrounded by the solid line) and the local electrons  $\rho_i^{2nd}(r)$  (two spherical symmetric distribution around each nucleus surrounded by the dashed lines) when two ions come together in a hot and dense plasma.

and the ion sphere radius of each ion shown by the two dashed line circles in Fig. 1 remain unchanged. In order to have the density of the nonlocal free-electron sea unchanged, when the two ions become overlapped, the boundary shown by the solid line changes in such a way that the truncated spherical volume surrounded by the solid line equal to the sum of the two separated ions to keep the electrical neutrality in the whole interaction region. Thus, the total density is  $\rho = \rho_A^{2nd} + \rho_B^{2nd} + \rho(r_b)$ . Figure 2 gives the electronic charge distribution of the two interacting Al atoms calculated in the present scheme and in the full-potential linearized augmented plane-wave (FLAPW) approach [26]. One can find that the delocalized electrons are rearranged and occupy the space between the two atoms; however, the localized electrons do not change when one puts the two atoms together. The figure supports the treatment that only delocalized electrons are rearranged when the nuclei come closer.

The pair potentials are computed under two main assumptions: (i) when two ions come closer, the local electronic densities around the nuclei obtained by using the AA model with ion sphere radius determined by the macroscopic plasma density and temperature are considered not to be

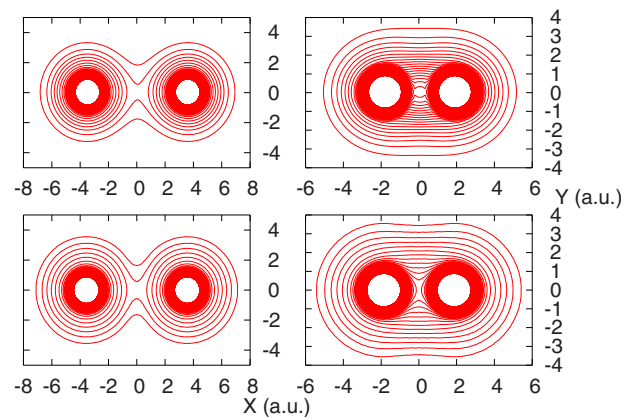


FIG. 2. (Color online) The electronic charge distribution of the two Al atoms calculated with the full-potential linearized augmented plane-wave (FLAPW) model (top) and the present model (bottom) with two interatomic separations. The curves are the constant curves of the electronic density.

arranged; and (ii) the potential consists of the static Coulomb interaction  $V_{Coul}(R)$ , the kinetic  $V_k(R)$ , the exchange  $V_e(R)$ , and the correlation  $V_c(R)$  energies:

$$V(R) = V_{Coul}(R) + V_k(R) + V_e(R) + V_c(R), \quad (1)$$

where  $R$  is the distance between the two nuclei. They are the functionals of the electronic density  $\rho(r)$ . The static Coulomb potential can be calculated directly from electronic density according to the GK theory [21–23]. The difference between the present model and the original GK theory is that the electronic density of the isolated ion is divided into two parts: the electronic sea  $\rho(r_b)$  and the local electron  $\rho_i^{2nd}(r)$ . The kinetic  $E_k(\rho)$ , exchange  $E_e(\rho)$ , and correlation  $E_c(\rho)$  energy densities [21,22,24,27,28] have been computed approximately only based on the electron densities in the spheroidal coordinate system,  $\lambda_1 = (r_1 + r_2)/R$ ,  $\lambda_2 = (r_1 - r_2)/R$ . Considering the effect of the temperature, the energy densities are expressed as

$$E_k(\rho) = \frac{\sqrt{2}}{\pi^2 \rho} \int \frac{\epsilon^{3/2}}{\exp[(\epsilon - \mu)/T] + 1} d\epsilon, \quad (2)$$

where the chemical potential  $\mu$  is obtained using the requirement  $\rho = \frac{\sqrt{2}}{\pi^2} \int \frac{\epsilon^{1/2}}{\exp[(\epsilon - \mu)/T] + 1} d\epsilon$  at a space point with total electronic density  $\rho$  and therefore the nonlinear changes in the occupancies and kinetic energy with the electron density are considered:

$$E_e(\rho) = -0.6109r_s^{-1} \times \frac{1 + 2.83431t^2 - 0.21512t^3 + 5.27586t^4}{1 + 3.94309t^2 + 7.91379t^4} \tanh(t^{-1}) \quad (3)$$

and

$$E_c(\rho) = -0.6109r_s^{-1/2} \times \frac{-0.0081 + 1.127t^2 + 3.756t^4}{1 + 1.291t^2 + 3.593t^4} \tanh(t^{-1/2}), \quad (4)$$

where the  $r_s = 0.6203474\rho^{-1/3}$  and  $t = 0.543r_s^2 T$ ;  $T$  is the temperature. The total energy of the interaction system reverts back to the sum of the component energies automatically when the separation is greater than the sum of the two ion sphere radii. Therefore, the potential energy is defined as the total energy minus those of the separate atoms or ions, so when the two atoms or ions do not overlap, the interaction potential goes to zero:

$$V_k(R) = \pi \int \int d\lambda_1 d\lambda_2 r_1 r_2 \times \{\rho E_k(\rho) - \rho_A E_k(\rho_A) - \rho_B E_k(\rho_B)\}, \quad (5)$$

$$V_e(R) = \pi \int \int d\lambda_1 d\lambda_2 r_1 r_2 \times \{\rho E_e(\rho) - \rho_A E_e(\rho_A) - \rho_B E_e(\rho_B)\}, \quad (6)$$

$$V_c(R) = \pi \int \int d\lambda_1 d\lambda_2 r_1 r_2 \times \{\rho E_c(\rho) - \rho_A E_c(\rho_A) - \rho_B E_c(\rho_B)\}, \quad (7)$$

where  $\rho(r)$  are equal to  $\rho_A^{2nd}(r) + \rho_B^{2nd}(r) + \rho(r_b)$  with  $A$  and  $B$  labeling the two nuclei, respectively. The integrations over  $\lambda_1$  and  $\lambda_2$  are carried out using the Gaussian-Legendre numerical quadratures.

The separate electron densities are calculated in a full relativistic self-consistent field AA model, which is one of the statistical approximations applied to calculations of the electronic structure of atoms and ions in hot and dense plasmas based on the statistical average over the details of the populations of ions and occupations of the electronic energy levels [5–8]. The influence of the environment on the atom is assumed to have spherical symmetry on average. The movement of an electron under the interactions of the nucleus and other electrons is approximated by a central field, which is determined with the self-consistent calculation. However, in the region of strongly coupled plasmas, ion-ion pair interactions will break the spherically symmetric ionic potential and affect the electronic distributions. Considering these effects, we have treated the bound energy levels in the AA model as the energy bands with a Gaussian distribution of the density of states, which is normalized to ensure that the integration of the density of states over one band is equal to the statistical weight of the corresponding atomic level. The results affect greatly the ionization and equation of state [25,29]. The free electrons are considered more simply with an assumption of the temperature-dependent TF [1–3] treatment.

According to the computation of electron density using the modified AA model, we conclude that the nonlocal free-electron density depends only on the local potential, temperature, and chemical potential, as the local potentials at the ion sphere boundary in plasma should be a continuum, even in mixtures [8]. So the average nonlocal free-electron density at the ion sphere boundary should be the same in the equilibrium plasma. In fact, the electron density across the ion sphere boundary varies smoothly and only near the nucleus changes sharply. Therefore, it is reasonable that we divided the electron distribution into two parts: the uniformly distributed nonlocal free-electronic sea in the whole space with a density equal to the total electron density at the ion sphere boundary and the localized electrons around each nucleus, whose distribution is the total density minus the density of the nonlocal free-electronic sea and does not change when two interacting ions come together. On the basis of the pair potentials obtained above, the ion distribution is simulated using the classical molecular dynamics (MD) scheme. As an example, Fe and Al equations of state and ion distribution are given at a wide region of density and temperature. The AA model is, in particular, suitable for a description of the electron distribution in hot and dense matters. Therefore, the present approach can be applied to the temperature and density regions where the *ab initio* molecular dynamics technique [9] is difficult to apply due to the numerical difficulties.

### III. RESULT AND DISCUSSION

In plasmas, the pair potentials are calculated according to the temperature- and density-dependent electron densities

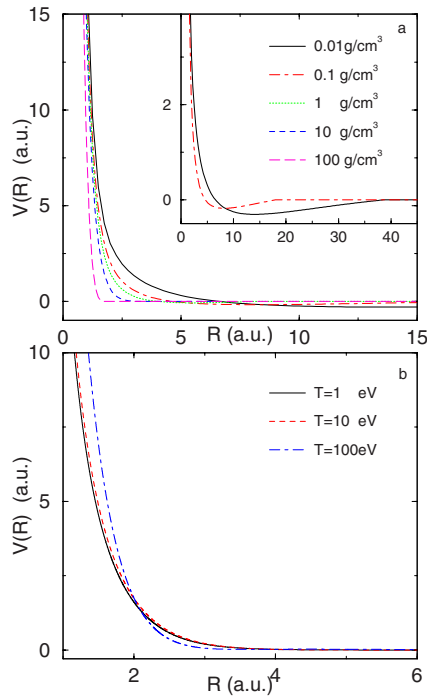


FIG. 3. (Color online) The ion-ion pair potentials in Al plasmas: (a) at  $T=10$  eV and densities  $0.01$ ,  $0.1$ ,  $1$ ,  $10$ , and  $100 \text{ g/cm}^3$  and (b) at density  $5 \text{ g/cm}^3$  and  $T=1$  eV (solid line),  $10$  eV (dashed line), and  $100$  eV (dot-dashed line).

around the nucleus. First, we give the results of Al at the temperature of  $10$  eV and a few different densities of plasma in Fig. 3(a), from which one can find that the pair potential becomes zero when the distance of two ions is larger than the sum of their radii as the polarization and dispersion effects are not included in the present model. In order to consider the density effects, an AA model for electrons confined within a limited average size ion sphere is employed [8,25]. Within each ion sphere, the charge neutrality is retained by having the total electron (nonlocal plus local) number equal to the nuclear charge. Therefore, the direct Coulomb interaction potential will be zero due to the screening of electrons, and the exchange, kinetic, and correlation potentials calculated with the LDA will also be zero without density overlap between the ions. So the present model would be more adequate to describe the short-range pair repulsive potentials between ions in hot and dense matter. One can also find the apparent density effects on the pair potentials: the higher the density is, the weaker the repulsion of the pair potential when the two ions begin to overlap in space. Except for the  $0.01$  and  $0.1 \text{ g/cm}^3$  cases, the ionizations of the electrons in  $1$ ,  $10$ , and  $100 \text{ g/cm}^3$  plasmas are mainly caused by the pressure ionization; i.e., the higher the material density is, the more the electrons are ionized. The repulsion between the ions is mainly from the increase of the kinetic energy due to the Pauli principle, which depends on the overlap of the electron density between the interacting ions, and the Coulomb repulsion between the nuclei, which depends on the screening of the electrons. With more nonlocal ionized electrons, the significance of both the density overlap and screening would be reduced, resulting in a weaker repulsion between

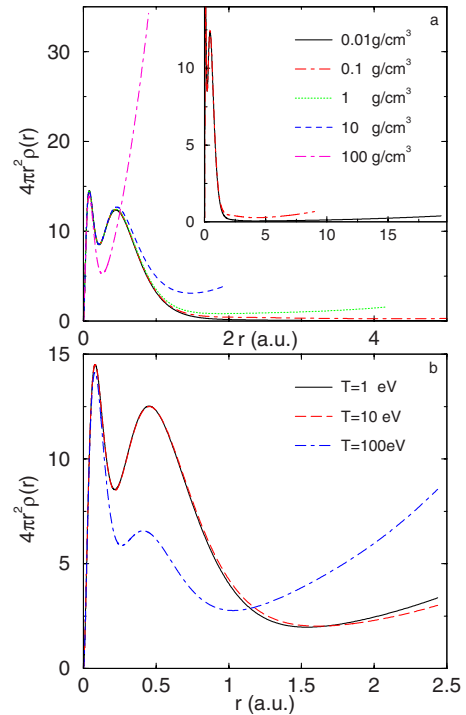


FIG. 4. (Color online) The radial distributions of the electron densities: (a) at  $T=10$  eV and densities  $0.01$ ,  $0.1$ ,  $1$ ,  $10$ , and  $100 \text{ g/cm}^3$  and (b) at density  $5 \text{ g/cm}^3$  and  $T=1$  eV (solid line),  $10$  eV (dashed line), and  $100$  eV (dot-dashed line).

the ions. The radial electron density distribution with different densities of plasma is shown in Fig. 4(a); one can find that the nonlocal ionized electron density at the ion sphere boundary gets the highest value for  $100 \text{ g/cm}^3$  plasma. The pair potentials in Fig. 3(a) become almost the same when the two ions come closer because the nuclear repulsion dominates the interaction at very small distances. In addition, the pair potentials of  $100 \text{ g/cm}^3$  are almost the same as the hard-sphere potential because the plasma density is very high and the free space for the ion motion is very small, and when two ions come closer, the interaction will be increasing rapidly. One can see that the potentials at the densities of  $0.01$  and  $0.1 \text{ g/cm}^3$  have a shallow well to show that at these densities the gas has negative cold pressure. Second, in Fig. 3(b) the Al pair potentials of  $5 \text{ g/cm}^3$  at temperatures of  $1$ ,  $10$ , and  $100$  eV are given. From the figure, it can be seen that the potentials at temperatures of  $1$  and  $10$  eV have little difference; however, a greater difference appears at  $100$  eV. The reason is similar to that accounting for the differences shown in Fig. 3(a)—i.e., the differences in the density of the nonlocal free electrons. With the density  $5 \text{ g/cm}^3$ , at  $1$  and  $10$  eV only the  $3s$  and  $3p$  electrons are ionized and the distribution of the local electron densities around the nuclei changes little from  $1$  eV to  $10$  eV. At  $100$  eV, most  $2p$  electrons have been ionized thermally and the distributions of local and nonlocal electrons have considerable differences with those of  $1$  eV and  $10$  eV. The radial distributions of the electron densities at  $1$ ,  $10$ , and  $100$  eV are shown in Fig. 4(b), which give a clear correlation between the temperature dependence of the pair potentials and the electron distributions. When two ions come closer than about  $2$  a.u., compared to  $1$  and

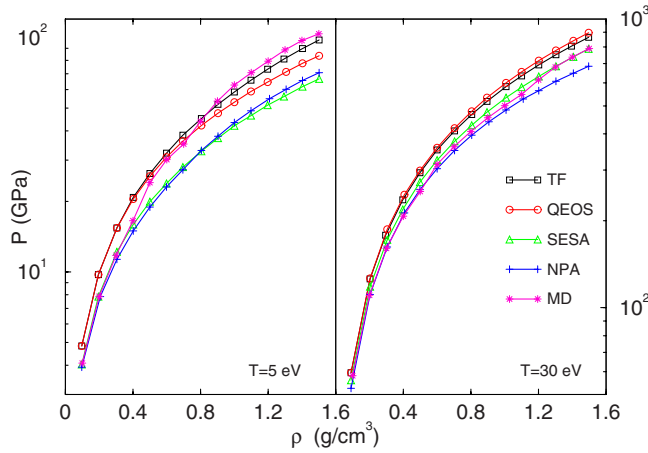


FIG. 5. (Color online) The calculated equations of state at  $T = 5$  and  $30$  eV and densities  $0.1 < \rho < 1.5$  g/cm<sup>3</sup> compared with the results of TF, QEOS, SESA, and NPA given in Ref. [31].

10 eV, the influence of the reduced electronic screening on the Coulomb interaction between the two nuclei exceeds the influence of the reduced Pauli exclusion principle on the kinetic energy; the repulsive interaction at 100 eV is stronger than those at 1 eV and 10 eV.

As an example, classical MD simulations are made at temperatures of 5 eV and 30 eV and densities of  $0.1 < \rho < 1.5$  g/cm<sup>3</sup> on the basis of the above pair-potential calculations. A number of 4000 ions are included to make the MD simulations with the  $NVT$  (constant  $N$ , number of particles;  $V$ , volume; and  $T$ , temperature) ensemble and the periodic boundary conditions being applied [30]. Each MD simulation consists of two stages: the equilibration stage and the productive stage. At the productive stage, the physical properties of the matter are obtained by averaging over the time period of the stage. The results of MD simulations in the  $NVT$  ensemble depend on the number of time steps,  $n_t$ ; size of the time step,  $t$ ; number of ions,  $N$ ; and the cutoff  $r_{cutoff}$ . It is found that correct results can be obtained with  $n_t = 200\,000$ ,  $r_{cutoff} = 2r_{ws}$ , where the average sphere volume equal to  $\frac{1}{n_i} = \frac{4}{3}\pi r_{ws}^3$  and  $n_i$  is the ion number density of the plasma.  $t$  is determined by the plasma temperature and density. The initial configurations of the ions are set as the ideal fcc crystal structure. We extract the thermodynamic parameters from the simulations by using the classical virial expressions, such as  $PV = NK_B T + \frac{1}{3} \langle \sum_i x_i \frac{\partial U}{\partial x_i} \rangle$ . The electronic pressure is calculated from the modified AA model [25,29]. We first make comparisons of the calculated equations of state (EOS) of Al with the results given by Perrot *et al.* [31] in Fig. 5. Their results were obtained with the TF model [3], the quotidian equations of states (QEOS) model [32], the SESAME (SESA) databases [33], and the neutral pseudoatom (NPA) model [31], respectively. The behaviors at 30 eV and 5 eV are very similar with the EOS of the TF, QEOS, SESA, and NPA models in Ref. [31]. Especially, our results agree well with those of NPA and SESA at 30 eV, for which the electrons in the NPA model are described in the framework of DFT and the ion correlations are described by using the HNC method, and the SESA EOS is an interpolation among the results of several theories valid in adjacent domains. The

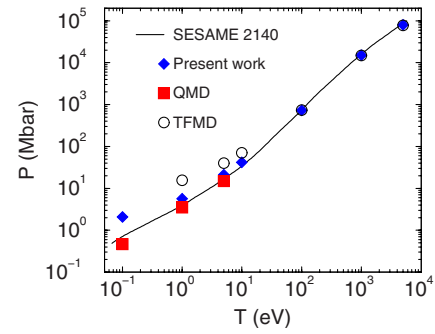


FIG. 6. (Color online) The principal Hugoniot of iron. The line is the SESAME EOS No. 2140, diamonds are present results, squares are the QMD results, and circles are the TFMD results.

results at 5 eV and high densities are larger due to the pressure ionization of  $3s$  electrons.

In order to examine the present model over a large range of temperature and density, we calculate the iron equation of state and the ionic structure. Molecular dynamics simulations are performed as above. In Fig. 6, we first give the Fe principal Hugoniot curve and make comparisons between our results and the SESAME EOS No. 2140 data, quantum molecular dynamics (QMD) result, and TFMD results given in Ref. [17]. At a high temperature, our results are in good agreement with that of SESAME EOS No. 2140 and TFMD. When the temperatures are smaller than 10 eV, our results are smaller than the TFMD ones because our model includes the electronic exchange energy parts [34] and electronic shell structures and larger than those of the SESAME EOS No. 2140 and the QMD because of the larger electronic pressure in the present model.

In Fig. 7, we show the ion-ion pair distribution functions (PDFs) at 10 eV, 100 eV, 1000 eV, and 5000 eV and make comparisons with those of TFMD and the one-component plasma (OCP) [17]. The PDFs show that our nearest-

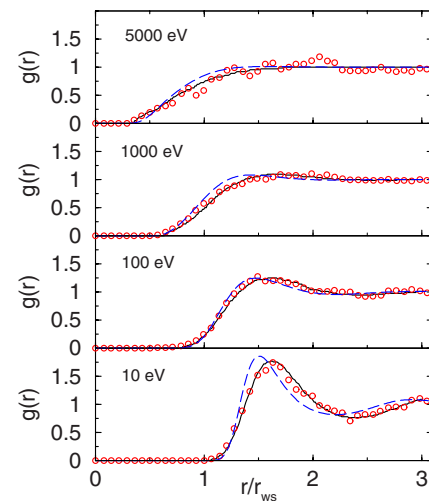


FIG. 7. (Color online) The Fe ion-ion pair distribution functions at the temperatures and densities of (10 eV, 22.5 g/cm<sup>3</sup>), (100 eV, 34.5 g/cm<sup>3</sup>), (1000 eV, 39.65 g/cm<sup>3</sup>), and (5000 eV, 34.37 g/cm<sup>3</sup>). The dashed lines are the present results, the circles are the TFMD results, and the solid lines are the OCP results.

neighbor distances are slightly larger than those of TFMD and OCP; in particular, the discrepancy becomes notable at 10 eV. In fact, for our model at low temperature very few electrons are thermally ionized and most of them are localized around the nuclei, and when two nuclei come together, they will have more electronic clouds overlapped and we will obtain a stronger repulsive interaction. So at low temperatures we should consider the electronic relaxations during the interaction and obtain more reasonable pair potentials or apply first-principles QMD methods.

#### IV. CONCLUSION

An alternative molecular dynamics simulation scheme, which can be applied to hot and dense plasmas over a wide

range of temperature and density, is proposed by combining the AA model for electron description and a modified GK model for interionic pair potentials. As numerical examples, the EOS of Al and Fe and the ion-ion pair distribution functions are calculated by carrying out molecular dynamics simulations based on the calculated pair potentials. It is shown that the results are in reasonable agreement with other theoretical models and, in particular, with the SESAME database.

#### ACKNOWLEDGMENTS

This work was supported by the National Natural Science Foundation of China under Grant No. 10734140, the National Basic Research Program of China (973 Program) under Grant No. 2007CB815105, and the National High-Tech ICF Committee in China.

- 
- [1] L. H. Thomas, Proc. Cambridge Philos. Soc. **23**, 542 (1927); E. Fermi, Z. Phys. **48**, 73 (1928).
- [2] R. P. Feynman, N. Metropolis, and E. Teller, Phys. Rev. **75**, 1561 (1949).
- [3] R. Latter, Phys. Rev. **99**, 1854 (1955).
- [4] P. A. M. Dirac, Proc. Cambridge Philos. Soc. **26**, 376 (1930).
- [5] B. F. Rozsnyai, Phys. Rev. A **5**, 1137 (1972); J. Quant. Spectrosc. Radiat. Transf. **27**, 211 (1982); B. F. Rozsnyai and M. Lamoureux, *ibid.* **43**, 381 (1990).
- [6] G. Faussurier, C. Blancard, and A. Decoster, Phys. Rev. E **56**, 3474 (1997); **56**, 3488 (1997).
- [7] D. A. Liberman, Phys. Rev. B **20**, 4981 (1979); J. Quant. Spectrosc. Radiat. Transf. **27**, 335 (1982).
- [8] J. Yuan, Phys. Rev. E **66**, 047401 (2002).
- [9] R. Car and M. Parrinello, Phys. Rev. Lett. **55**, 2471 (1985).
- [10] S. Mazevet, F. Lambert, F. Bottin, G. Zérah, and J. Clérouin, Phys. Rev. E **75**, 056404 (2007).
- [11] M. W. C. Dharma-wardana and Francois Perrot, Phys. Rev. A **26**, 2096 (1982).
- [12] M. W. C. Dharma-wardana and Michael S. Murillo, Phys. Rev. E **77**, 026401 (2008).
- [13] Dror Ofer, E. Nardi, and Y. Rosenfeld, Phys. Rev. A **38**, 5801 (1988).
- [14] H. Furukawa and K. Nishihara, Phys. Rev. A **46**, 6596 (1992).
- [15] G. Zérah, J. G. Clérouin, and E. L. Pollock, Phys. Rev. Lett. **69**, 446 (1992).
- [16] J. Clérouin, E. L. Pollock, and G. Zérah, Phys. Rev. A **46**, 5130 (1992).
- [17] Flavien Lambert, Jean Clérouin, and Gilles Zérah, Phys. Rev. E **73**, 016403 (2006).
- [18] J.-F. Danel, L. Kazandjian, and G. Zérah, Phys. Plasmas **13**, 092701 (2006); **15**, 072704 (2008).
- [19] D. Salzmann and D. V. Fisher, High Energy Density Phys. **3**, 242 (2007).
- [20] B. F. Rozsnyai, J. R. Albritton, D. A. Young, V. N. Sonnad, and D. A. Liberman, Phys. Lett. A **291**, 226 (2001).
- [21] R. G. Gordon and Y. S. Kim, J. Chem. Phys. **56**, 3122 (1972).
- [22] Y. S. Kim and R. G. Gordon, Phys. Rev. B **9**, 3548 (1974).
- [23] A. J. Cohen and R. G. Gordon, Phys. Rev. B **12**, 3228 (1975); **14**, 4593 (1976).
- [24] Jianmin Yuan, Yijun Zhao, and Zhijie Zhang, Acta Mech. Sin. **21**, 479 (1989) (in Chinese).
- [25] Yong Hou, Fengtao Jin, and Jianmin Yuan, Phys. Plasmas **13**, 093301 (2006).
- [26] P. Blaha, K. Schwarz, G.-K. Madsen, D. Kvasnick, and J. Luitz, WIEN2K, an augmented plane wave plus local orbitals program for calculating crystal properties, Vienna University of Technology, Vienna, 2002.
- [27] J. C. Slater, *Quantum Theory of Atomic Structure Vol. II* (McGraw-Hill, New York, 1960).
- [28] W. J. Carr, R. A. Coldwell-Horsfall, and A. E. Fein, Phys. Rev. **124**, 747 (1961); W. J. Carr and A. A. Maradudin, Phys. Rev. **133**, A371 (1964).
- [29] Yong Hou, Fengtao Jin, and Jianmin Yuan, J. Phys.: Condens. Matter **19**, 425204 (2007).
- [30] M. P. Allen and D. J. Tildesley, *Computer Simulation of Liquids* (Clarendon, Oxford, 1987).
- [31] F. Perrot, M. W. C. Dharma-Wardana, and J. Benage, Phys. Rev. E **65**, 046414 (2002).
- [32] R. M. More, K. H. Warren, D. A. Yong, and G. B. Zimmerman, Phys. Fluids **31**, 3059 (1988).
- [33] K. Trainor, in *Handbook of Material Properties Data Bases*, edited by W. Huebner (Los Alamos National Laboratory, Los Alamos, 1984), Vol. Ic, p. 3712.
- [34] P. Fromy, C. Deutsh, and G. Maynard, Phys. Plasmas **3**, 714 (1996).